Nuclear Fusion in Stars: Origin of the Elements

C. Iliadis*
Department of Physics & Astronomy, University of North Carolina at Chapel Hill, Chapel Hill, North Carolina, 27599, USA

Half a century has passed since the foundation of nuclear astrophysics. Today, nuclear astrophysics represents a multidisciplinary field that combines achievements in theoretical astrophysics, observational astronomy, cosmochemistry and nuclear physics. New tools and developments have revolutionized our understanding of the origin of the elements: supercomputers have provided astrophysicists with the required computational capabilities to study the evolution of stars in a multidimensional framework; the emergence of high-energy astrophysics with space-borne observatories has opened new windows to observe the Universe; cosmochemists have isolated small pieces of stardust embedded in primitive meteorites providing clues regarding processes operating in stars; and nuclear physicists have measured reactions near stellar energies through the combined efforts using stable and radioactive-ion beam facilities. This contribution will explain fundamental aspects of nuclear reactions in stars, with examples taken from thermonuclear explosions in classical novae and helium burning in AGB and massive stars.

1. Introduction

Life on Earth depends on nuclear processes deep inside the Sun. But how exactly the nuclear transmutations occur was not understood for some time. The breakthroughs came at the end of the 1930's: Bethe and Critchfield [1] uncovered a sequential reaction sequence fusing hydrogen (H) to helium (He), now referred to as the "pp1 chain", while Bethe [2] and von Weizsäcker [3] proposed a cyclic reaction sequence, now called the "CNO1 cycle", that has the same end result of synthesizing He from H. For this early work, the Nobel prize was awarded to Hans Bethe in 1967. It is interesting to point out that in those days it was thought the Sun derives most of its energy via the CNO1 cycle. Part of the problem was that some of the key nuclear reaction cross sections were poorly known. When more reliable cross sections could be estimated in the 1950's, it became apparent that it is in fact the pp1 chain that governs the energy production in the Sun. The important lesson is that accurate nuclear physics information is crucial for our understanding of stars.

Some obvious questions followed immediately. How do other stars produce energy? How do they evolve and why do some of them explode? And perhaps the key question: what is the origin of the elements? They were certainly not produced inside the Sun and, therefore, other processes are required to explain their origin. A major breakthrough was achieved with the detection of technetium in the spectra of several S stars by Merrill [4] in the early 1950's. Since this particular element has no stable isotopes and the radioactive technetium isotopes have rather short half-lives on a Galactic time scale, the obvious conclusion was that the technetium must have been produced in the observed stars and thus nucleosynthesis must still be going on in the Galaxy. Another aspect of paramount importance in this regard was the observed solar system abundance distribution. It is displayed in Fig. 1 and reveals a rather complicated structure. The different processes giving rise to the observed features were explained by Burbidge, Burbidge, Fowler and Hoyle [5] and by Cameron [6]. These papers laid the foundation of the modern theory of nuclear astrophysics. For this work, the Nobel prize was awarded to Willy Fowler in 1983.

Briefly, H and He are the most abundant species and are mainly produced in the Big Bang. The abundance curve then drops

*Electronic address: iliadis@unc.edu

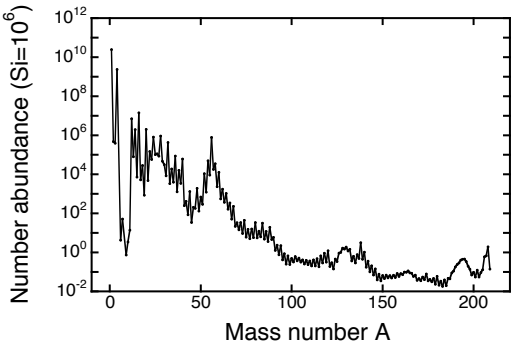

FIG. 1: Abundances of the nuclides, normalized to the number of Si atoms, at the birth of the solar system. Data from Ref. [7].

sharply by several orders of magnitude. The species ^{6}Li, ^{9}Be and B are so quickly destroyed inside stars that their production must take place elsewhere. In fact, they are believed to be produced by cosmic-ray spallation. The abundance curve increases sharply at C and O. These are the most abundant elements after H and He and, incidentally, are the species life on Earth is based on. For increasing mass number the abundance curve decreases, but then produces a maximum near Fe, Co and Ni, referred to as the *iron peak*. Interestingly, these nuclides exhibit the largest binding energies per nucleon. So far, most of the species have been produced by nuclear reactions involving charged particles. To explain the origin of the nuclides located beyond the iron peak, however, fundamentally different processes are required. Those species are mainly produced via the capture of neutrons by the astrophysical *s-process* and *r-process*.

All nuclides heavier than boron are made in stars. At the end of their lives, stars eject their nuclear ashes into space. Out of this matter new generations of stars are born and a new cycle of nuclear transmutations is initiated. Without the occurrence of the many nuclear processes in primordial and stellar nucleosynthesis, the universe would be a dark and chemically poor place. Certainly, no form of life as we know it could have ever emerged. In the following some key nuclear physics aspects are explained in order to appreciate nuclear fusion in stars. In addition, some recent nuclear laboratory work is discussed, with examples taken from thermonuclear explosions in classical novae and helium burning in AGB and massive stars.

2. Nuclear reactions

The cross section of a nuclear reaction is defined as the number of interactions per time, divided by the number of incident particles per area and time, and divided by the number of target nuclei within the beam. The unit is *barn*, where 1 barn$\equiv 10^{-28}$ m^2. For example, the estimated cross section for the reaction $p+p \rightarrow d+e^+ +\nu$, which represents the first step in the pp chains, amounts to $\sigma = 8\times10^{-48}$ cm^2 at a laboratory bombarding energy of 1 MeV. Suppose a measurement of this reaction would be performed using an intense 1 mA beam of protons, incident on a dense hydrogen target (10^{20} protons per cm^2), then one obtains only 1 interaction in 6000 years! Clearly, such a measurement is beyond present experimental capabilities and hence this cross section needs to be estimated theoretically.

Cross section curves (cross section versus bombarding energy) come in many varieties. In the simplest case, the cross section of a charged-particle reaction drops dramatically with decreasing energy, but otherwise exhibits no structure. A good example is the cross section for ^{16}O(p,γ)^{17}F below a center of mass energy of 2 MeV. Sometimes the cross section exhibits a well-defined maximum. An example for such a behavior is the ^{13}C(p,γ)^{14}N reaction, which shows a maximum near 500 keV in the center of mass.

The Coulomb barrier is responsible for the sharp drop in cross section with decreasing energy. The transmission coefficient for the Coulomb potential for low energies is given by

$$\hat{T} \approx \exp\left(-\frac{2\pi}{\hbar}\sqrt{\frac{m_{01}}{2E}}Z_0 Z_1 e^2\right) \equiv e^{-2\pi\eta} \quad (1)$$

where m_{01} is the reduced mass, Z_0 and Z_1 are the charges of the interacting nuclei and e is the elementary charge. This function reveals a $1/\sqrt{E}$ dependence in the exponent

and is referred to as the *Gamow factor*. It is frequently used in nuclear astrophysics to define a rather useful quantity, called the astrophysical S-factor, via the relation $S(E) \equiv E\sigma(E)\exp(2\pi\eta)$: division by the Gamow factor removes from the cross section, $\sigma(E)$, the strong Coulomb barrier transmission probability and produces a function, $S(E)$, that is more manageable (for example, in theoretical extrapolations to very low energies).

On the other hand, cross section maxima are identified as *resonances*. In formal reaction theory, a simple equation describing a single isolated resonance can be derived. It is referred to as *Breit-Wigner formula* and is given by

$$\sigma_{\rm BW}(E) = \frac{\lambda^2\omega}{4\pi}\frac{\Gamma_a\Gamma_b}{(E_r-E)^2+\Gamma^2/4} \qquad (2)$$

where λ is the de Broglie wavelength, ω is a factor containing angular momenta, E_r is the resonance energy, Γ_i are the resonance partial widths of entrance and exit channel, and Γ is the total resonance width given by the sum of all partial widths. The above equation is the single most important expression describing a resonance and it is frequently used in nuclear astrophysics in many applications [8].

3. Thermonuclear reactions

In a stellar plasma, the kinetic energy for a nuclear reaction derives from the thermal motion of the participating nuclei. Hence, the interaction is referred to as *thermonuclear reaction*. The thermonuclear reaction rate (the number of reactions per unit time and unit volume) for a reaction $0+1 \rightarrow 2+3$ is given by $r_{01} = N_0 N_1 \langle\sigma{\rm v}\rangle_{01}$, where N_i are the number densities of the interacting nuclei and $\langle\sigma{\rm v}\rangle_{01}$ is the reaction rate per particle pair, which is equal to the integral over the product of cross section and velocity probability density. In most cases of practical interest, the latter function is given by the Maxwell-Boltzmann distribution. Thus the reaction rate per particle pair can be written as

$$\langle\sigma{\rm v}\rangle_{01} = \frac{const}{(kT)^{3/2}}\int_0^\infty E\,\sigma(E)\,e^{-E/kT}\,dE \qquad (3)$$

with $const = \sqrt{8/(\pi m_{01})}$; k the Boltzmann constant, and T the plasma temperature. Clearly, for a given temperature the reaction rate is precisely determined if the nuclear reaction cross section, $\sigma(E)$, is known.

It is worthwhile to note that a given nuclear reaction occurring in the stellar plasma can rarely be considered as an isolated interaction. Consider, for example, the species ^{25}Al at an elevated temperature. It may be destroyed in several different ways: via β^+-decay to ^{25}Mg, via proton capture to ^{26}Si, via photodisintegration to ^{24}Mg, and so on. On the other hand, ^{25}Al is produced via the β^+-decay of ^{25}Si, via proton capture on ^{24}Mg, via photodisintegration of ^{26}Si, and so on. The abundance evolution of ^{25}Al during nucleosynthesis is then given by a differential equation that accounts for all destruction and production mechanisms. Of course, such a differential equation needs to be written for all species participating in the nuclear burning. Thus one obtains a system of coupled differential equations, called a *nuclear reaction network*, which can be solved numerically [9].

It is interesting to investigate Eq. (3) in more detail by considering two extreme examples. The simplest case is a nearly constant S-factor, S_0. This situation is usually referred to as "non-resonant", which however leads to considerable misunderstandings since the formalism also applies to slowly varying resonance "tails". Substitution of the S-factor definition (see above) into Eq. (3) shows immediately that the reaction rate depends, apart from the magnitude of S_0, on the integral over the product of Gamow and Boltzmann factors, $e^{-2\pi\eta}e^{-E/kT}$. This result is significant because it demonstrates that the star does not burn at high energies where the cross section is large (since the number of particles with such energies is vanishingly small); neither does the star burn at very small energies where the number of particles is at maximum (since the cross section is vanishingly small). Rather, in a plasma most nuclear reactions occur at energies where the function $e^{-2\pi\eta}e^{-E/kT}$ is at maximum. This well-defined energy window is referred to as the *Gamow peak*.

When the Gamow peak is plotted for a given temperature, but for different target-projectile combinations (implying different projectile and target charges and hence different Coulomb barrier heights), a few important observations can be made. For increasing charges Z_0 and Z_1: (i) the Gamow peak shifts to higher energies; (ii) the Gamow peak becomes broader; and most importantly, (iii) the area under the Gamow peak decreases dramatically. In other words, for a mixture of different nuclides in a stellar plasma at given temperature, those reactions with the smallest Coulomb barrier produce most of the energy and are consumed most rapidly. This is of paramount importance for the star since it explains the occurrence of well-defined stellar burning stages.

Next, we will consider a "narrow resonance". Several different definitions for a narrow resonance can be found in the literature, but none of them is without problems. For the sake of simplicity, let us assume that a narrow resonance implies constant partial widths over the total width of the resonance. Substitution of Eq. (2) into Eq. (3) yields immediately $\langle \sigma \mathrm{v} \rangle = [(2\pi)/(mkT)]^{3/2} \hbar^2 e^{-E_r/kT} \omega\gamma$. The product $\omega\gamma \equiv \omega\Gamma_a\Gamma_b/\Gamma$ is proportional to the area under the narrow-resonance cross section curve and thus is called *resonance strength* (with units of energy). Note that the resonance energy enters exponentially in the above reaction rate expression. It needs to be determined rather precisely, otherwise the resulting uncertainty of the reaction rate becomes relatively large.

In many cases the energy-dependence of the partial widths over the total width of the resonance cannot be disregarded. Such "broad resonance" reaction rates need to be treated with care. Although approximate expressions exist in the literature, it is safer to substitute Eq. (2) into Eq. (3) and evaluate the integral numerically. Depending on the location of the broad resonance with respect to the Gamow peak, there are in general two contributions to the total reaction rate. First, the contribution calculated from the "narrow resonance" reaction rate, which arises only from the region near the resonance energy (as is apparent from the factor $e^{-E_r/kT}$). Second, from the smoothly varying tail of the resonance. If the broad resonance is located outside the Gamow peak, then in most cases the resonance tail makes a far larger contribution than what is calculated from the narrow resonance expression. Plotting such reaction rates versus temperature frequently reveals a "kink" because the narrow resonance and broad resonance reaction rates have different temperature dependences.

Generally, in order to evaluate the total rate of a single reaction, many different contributions need to be taken into account: narrow and broad resonances, non-resonant processes, subthreshold resonances, cross section continua, interferences between different amplitudes, and so on. Every single reaction represents a special case and the evaluation process is usually tedious. Evaluations of reaction rates have been provided by Fowler and collaborators for many years, with their last evaluation (covering the A=1-30 target mass range) published in 1988 [10]. A European effort, by the NACRE collaboration, resulted in an updated reaction rate evaluation in 1999 [11], while another evaluation including for the first time radioactive target nuclei was published in 2001 [12].

4. Monte Carlo Reaction Rates

It is crucial for an experimentalist to understand the impact of a new measurement on the derived reaction rates. However, the procedures that we have applied until very recently lack any statistical meaning. This may come as a surprise, but reflects reality: what is the precise meaning of a published recommended reaction rate? How are we to interpret a published lower or upper rate "limit"? And what is the probability density function of a published reaction rate? None of these questions have clear answers using the commonly accepted procedures in nuclear astrophysics.

We have recently developed a Monte Carlo method of estimating reaction rates that will impact our field in a number of ways. A

simplistic example is given in Fig. 4, showing results for a single, hypothetical resonance in ^{22}Ne(α,γ)^{26}Mg (with an energy of E_r = 300±15 keV and a strength of $\omega\gamma = 4.1 \pm 0.2$ eV). Each of the two nuclear physics quantities is associated with a (input) probability density function. Random samples are drawn from each of these distributions and the resulting reaction rates are calculated according to the conventional formalism (analytical expressions or numerical integrations). The procedure is then repeated many times until the (output) reaction rate probability density function can be determined precisely (histogram in top part). The corresponding cumulative distribution (solid line in bottom part) is computed and the 16, 50 and 84 percentiles are determined, which are interpreted as low, recommended and high reaction rate, respectively. This simple example already reveals the power of the Monte Carlo method. The resulting rates have a statistical meaning: half of the samples lie below and half lie above the recommended rate, while the coverage probability between low and high rates amounts to 68%. Of course, the low and high rate boundaries can be determined according to any desired coverage probability.

The new Monte Carlo method is the foundation of a recently published thermonuclear reaction rate evaluation for A=14-40 targets [13–16]. The results show that the rates for many reactions have changed dramatically compared to previous results. It is obvious that the new Monte Carlo results not only quantify for the experimentalist the impact of a measurement, but they are of substantial interest to the stellar modeler as well since the reaction rate probability density function can directly be used to derive more reliable stellar model abundances. Experimental Monte Carlo reaction rates are now available for about 70 nuclear reactions. These results and methods form the backbone of a new library of nuclear interaction rates, called STARLIB, which our group has developed over the past few years. We anticipate the release of this next-generation data base at the end of 2012.

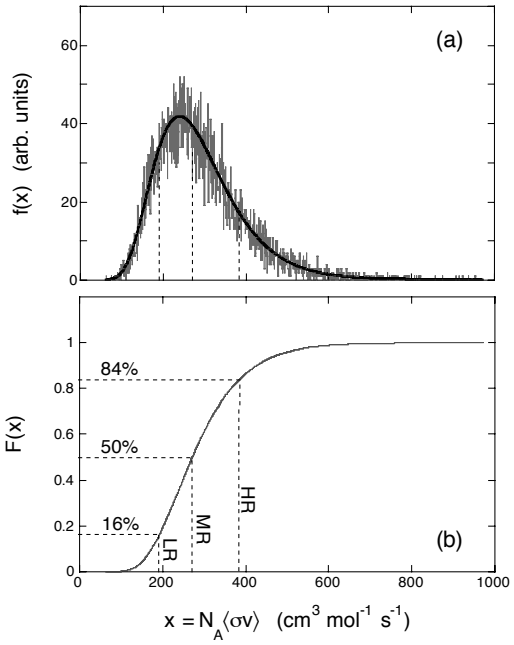

FIG. 2: Results of Monte Carlo rate calculation for a fictitious resonance in ^{22}Ne(α,γ)^{26}Mg at T=0.5 GK. (Top) Reaction rate probability density function, shown as grey histogram. (Bottom) Cumulative reaction rate distribution; the vertical dotted lines represent the low, median and high Monte Carlo reaction rates, which are obtained from the 16, 50 and 84 percentiles, respectively. The solid line in the top part shows a lognormal approximation of the actual Monte Carlo probability density function.

5. Direct Measurement of the $^{17}O + p$ Reaction for Classical Novae

The competing ^{17}O(p,γ)^{18}F and ^{17}O(p,α)^{14}N reactions at peak temperatures of $T = 0.1 - 0.4$ GK are of particular interest to classical novae since they are important for the Galactic synthesis of ^{17}O, the stellar production of radioactive ^{18}F, and for predicted oxygen isotopic ratios in presolar grains [17]. It has been demonstrated [18, 19] that the ^{17}O(p,γ)^{18}F reaction rate for classical nova conditions depends on the direct capture process, despite the fact that a narrow resonance (at a laboratory energy

of 193 keV) is located well inside the Gamow peak.

The existing low-energy data on the total S-factor in the ^{17}O(p,γ)^{18}F reaction are shown in Fig. 5. Four data points at bombarding energies between $E_{cm} = 280-425$ keV (shown as open full circles) have been reported by Rolfs [20]. The direct capture contribution derived in the analysis of Ref. [20] is shown as a dotted line. Furthermore, a total cross section measurement using an activation method has been reported by Chafa et al. [19] at a single, very low, energy of $E_{cm} = 180$ keV. This data point is shown as an open square in Fig. 5 and seems to agree with the direct capture S-factor reported by Rolfs [20]. However, it must be pointed out that its uncertainty amounts to ≈50% and hence the measurement is of limited significance only. Because the energy-dependence of the direct capture S-factor reported in Ref. [20] (shown as dotted line in Fig. 5) could not be reproduced, it was decided to remeasure the S-factor at low energies.

The experiment was carried out at the Laboratory for Experimental Nuclear Astrophysics (LENA), which is part of the Triangle Universities Nuclear Laboratory (TUNL). A 1 MV JN Van de Graaff accelerator supplied proton beams of up to 125 μA on target. Targets of ^{17}O were prepared by anodizing 0.5 mm thick tantalum backings in ^{17}O-enriched water. Prompt γ-rays from the ^{17}O(p,γ)^{18}F reaction were detected using a large-volume (582 cm^3) HPGe detector, placed at an angle of 55^o with respect to the proton beam direction and at a distance of 36 mm between detector front face and target midpoint.

The ^{17}O(p,γ)^{18}F reaction was measured at six bombarding energies and the resulting total S-factors are shown in Fig. 5 as full circles. The parameters of the dominant broad resonances at center of mass energies of 557 and 677 keV are well-known [21] and their contribution was subtracted from the total measured S-factor (solid line) in order to extract the direct capture contribution (shown as horizontal dashed line). We find a nearly energy-independent direct capture S-factor of

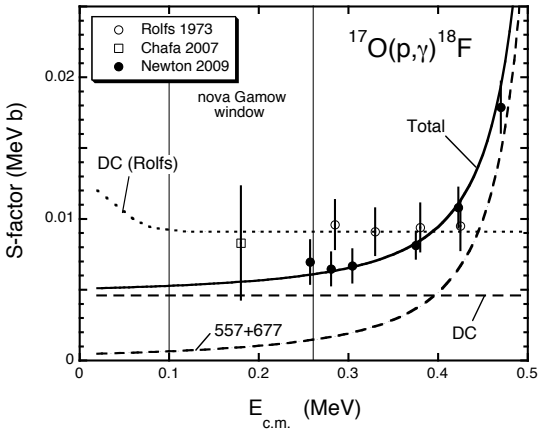

FIG. 3: World data on total, low-energy, non-narrow-resonant, S-factor in ^{17}O(p,γ)^{18}F. The previous data are shown as open symbols [19, 20], while the full circles display the new results of Newton et al. [22]. Two data points appear inside the nova Gamow peak region (for $T = 0.1 - 0.4$ GK). The solid line represents the sum of broad-resonance and newly determined direct capture contributions, while the dotted line shows the direct capture S-factor of Rolfs [20]. Note the factor of 2 difference between the direct capture predictions of Rolfs [20] (dotted line) and Newton et al. [22] (horizontal dashed line).

$S_{DC}(E) = 4.6$ keV b, which is a factor of about 2 lower than the prediction of Rolfs [20]. We also improved the uncertainty of the direct capture S-factor from an *assumed* value of ±50% in Ref. [18] to an *experimental* value of ±23% in our work. As already pointed out, the uncertainty on the data point from Ref. [19] is too large to be of any significance. With this new experimental information, Monte Carlo reaction rates for ^{17}O(p,γ)^{18}F have been computed and will be used in future hydrodynamical simulations of classical novae. For more detailed information, see Newton et al. [22].

6. Indirect measurement of the $^{22}Ne + \alpha$ Reaction for Massive Stars and AGB Stars

The ^{22}Ne+α reactions are important for the s(low neutron capture)-process in both mas-

sive stars and AGB stars. The neutrons that are produced by the ^{22}Ne(α,n)^{25}Mg reaction are captured by seed nuclei, unhindered by a Coulomb barrier, and give rise to the nucleosynthesis of about half of the elements beyond iron. In addition to this neutron source reaction, the competing ^{22}Ne(α,γ)^{26}Mg reaction is equally important since it removes α-particles that would otherwise be available for neutron production.

It is interesting to review the level structure in the ^{26}Mg compound nucleus between the α-particle threshold and the lowest-lying directly measured resonance at 840 keV bombarding energy. In total, there are 41 known levels of which only 3 are known to be of unnatural parity and thus can be excluded from further consideration. Of the remaining 38 states, only 13 were taken into account for calculating recently published reaction rates [23]. Obviously, more experimental work was required in order to derive a reliable rate. Of particular interest is a level at 11154 keV that was assigned a spin-parity of 1^- in the ^{26}Mg(γ,n) study of Berman et al. [24]. This state corresponds in energy to a resonance at 630 keV in the center of mass. An observation of this resonance was reported in Refs. [25, 26], but the signal was later shown to be caused by a contaminant reaction [27]. Since then the possible contribution of this expected resonance had a major impact on all of the published ^{22}Ne+α reaction rates. Thus we decided to determine unambiguously the spin-parities of ^{26}Mg states above and close to the α-particle threshold.

The experiment was carried out utilizing the linearly polarized, mono-energetic, γ-ray beam from the High Intensity γ-Ray (HIγS) facility, which is also part of the Triangle Universities Nuclear Laboratory (TUNL). More information on the HIγS facility can be found in Ref. [28]. The sample consisted of 16 g of MgO powder, enriched to 99.4% in ^{26}Mg, which was leased from Oak Ridge National laboratory. The polarized γ-ray beam incident on this sample had an energy between 10.8 and 11.4 MeV, corresponding to the excitation energy range to be covered in ^{26}Mg,

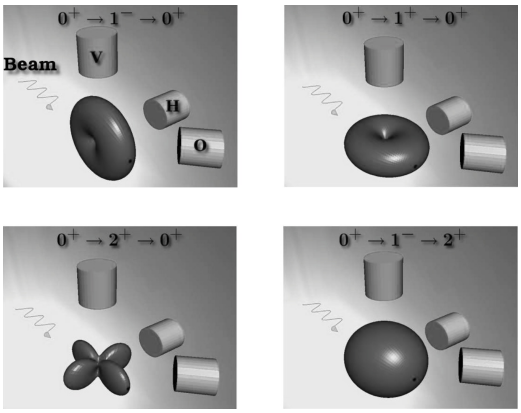

FIG. 4: Angular distributions of emitted photons expected from the ^{26}Mg nuclear resonance fluorescence experiment for different spin-parity sequences. The first and last spin-parity refers to the ground and final state in ^{26}Mg, respectively. The intermediate spin-parity refers to the ^{26}Mg level excited by the absorption of a photon from the incident γ-ray beam. The locations of the γ-ray detectors are also indicated ("V": vertical; "H": horizontal; "O": out of plane), while the ^{26}Mg sample was located at the center of the radiation patterns.

and a beam energy spread of ≈200 keV. The beam intensity at the sample position was about 10^7 photons per second. Scattered γ-rays from the sample were measured by several 60% HPGe counters that were positioned in the vertical plane, horizontal plane and out of plane, with respect to the incident beam direction. The setup is schematically shown in Fig. 6. The figure also shows the radiation pattern that results from the ^{26}Mg(γ,γ) reaction. Since the incident γ-ray beam is polarized, this type of angular distribution is referred to as "polarization-direction correlation". The radiation patterns shown in the figure were calculated using the formalism presented in Ref. [29].

It is interesting that different spin-parity sequences give rise to very different radiation patterns. The reverse statement also applies: measuring the radiation pattern of the scattered photons determines unambiguously the spin-parity of the excited intermediate level.

For example, the sequence $0^+ \rightarrow 1^- \rightarrow 0^+$ (upper left panel) refers to the excitation of a 1^- level from the 0^+ ground state of ^{26}Mg with a subsequent decay to a final state of 0^+. In this particular case no intensity is expected in the horizontal detector ("H") and maximum intensity should be observed in the vertical detector ("V"). The level corresponding to the elusive 630 keV resonance in ^{22}Ne+α was indeed observed in our experiment, but with maximum intensity in the horizontal detector and no intensity in the vertical detector, i.e., exactly the opposite of what is expected for a 1^- state. The important implication is that this level has a spin-parity of 1^+ ("unnatural parity") instead of 1^- and, consequently, cannot be formed in the ^{22}Ne+α reaction. Altogether we determined unambiguously the spin-parities for 5 levels near the α-particle threshold.

With this new experimental information, Monte Carlo reaction rates for ^{22}Ne(α,n)^{25}Mg and ^{22}Ne(α,γ)^{26}Mg have been computed. The new measurements give rise to a significant improvement in reaction rate uncertainties, yielding more accurate s-process abundance predictions for both AGB and massive star scenarios. More detailed information can be found in Longland et al. [30]. We are planning to use our new ^{22}Ne+α reaction rates in future hydrodynamical simulations of the s-process.

7. Summary

We reviewed several topics related to experimental and theoretical determinations of thermonuclear reaction rates. A new method of estimating experimental reaction rates using a Monte Carlo method has been presented. Apart from a median ("recommended") rate and high and low bounds, the complete reaction rate probability density function at any given temperature can now be derived. This new method is the foundation of our new evaluation of charged-particle thermonuclear reaction rates for A=14-40 target nuclei [14], and of our new library of nuclear interaction rates, called STARLIB, which has just been completed. Furthermore, the recent measurement of the ^{17}O(p,γ)^{18}F direct capture cross section at our LENA facility is presented. The results are important for the nucleosynthesis in classical novae, in particular, for the production of radioactive nuclei (mainly ^{18}F), for the Galactic origin of the nuclide ^{17}O, and for oxygen isotopic ratios in nova presolar grains. Also, we discussed the recent ^{26}Mg(γ,γ) study at our HIγS facility. The spins and parities of 5 levels near the α-particle threshold in ^{26}Mg could be determined, thus reducing significantly the rate uncertainties for the important s-process neutron source reactions ^{22}Ne(α,n)^{25}Mg and ^{22}Ne(α,γ)^{26}Mg in massive stars and in AGB stars.

Acknowledgments

This work was supported in part by the National Science Foundation under award number AST-1008355 and by the Department of Energy under grant number DE-FG02-97ER41041.

References

[1] H. A. Bethe, and C. L. Critchfield, *Phys. Rev.* **54**, 248 (1938).
[2] H. A. Bethe, *Phys. Rev.* **55**, 434 (1939).
[3] C. F. von Weizsäcker, *Phys. Z.* **39**, 633 (1938).
[4] P. W. Merrill, *Astrophys. J.* **116**, 21 (1952).
[5] E. M. Burbidge, G. R. Burbidge, W. A. Fowler, and F. Hoyle, *Rev. Mod. Phys.* **29**, 547 (1957).
[6] A. G. W. Cameron, *Pub. Astron. Soc. Pac.* **69**, 201 (1957).
[7] K. Lodders, *Astrophys. J.* **591**, 1220 (2003).
[8] C. Iliadis, *Nuclear Physics of Stars*, Wiley-VCH, Weinheim, 2007.
[9] D. Arnett, *Supernovae and Nucleosynthesis*, Princeton University Press, Princeton, 1996.
[10] G. R. Caughlan, and W. A. Fowler, *At. Data Nucl. Data Tab.* **40**, 284 (1988).
[11] C. Angulo, et al., *Nucl. Phys. A* **656**, 3 (1999).
[12] C. Iliadis, et al., *Astrophys. J. Suppl.* **134**, 151 (2001).

[13] R. Longland, C. Iliadis, A. E. Champagne, J. R. Newton, C. Ugalde, A. Coc, and R. Fitzgerald, *Nucl. Phys. A* **841**, 1 (2010).
[14] C. Iliadis, R. Longland, A. E. Champagne, A. Coc, and R. Fitzgerald, *Nucl. Phys. A* **841**, 31 (2010).
[15] C. Iliadis, R. Longland, A. E. Champagne, and A. Coc, *Nucl. Phys. A* **841**, 251 (2010).
[16] C. Iliadis, R. Longland, A. E. Champagne, and A. Coc, *Nucl. Phys. A* **841**, 323 (2010).
[17] C. Fox, C. Iliadis, A. E. Champagne, A. Coc, J. José, R. Longland, J. Newton, J. Pollanen and R. Runkle, *Phys. Rev. Lett.* **93**, 081102 (2004).
[18] C. Fox, C. Iliadis, A. E. Champagne, R. P. Fitzgerald, R. Longland, J. Newton, J. Pollanen and R. Runkle, *Phys. Rev. C* **71**, 055801 (2005).
[19] A. Chafa et al., *Phys. Rev. C* **75**, 035810 (2007).
[20] C. Rolfs, *Nucl. Phys. A* **217** (1973) 29.
[21] D.R. Tilley, H.R. Weller, C.M. Cheves and R.M. Chasteler, *Nucl. Phys. A* **595**, 1 (1995).
[22] J. R. Newton, C. Iliadis, A. E. Champagne, J. M. Cesaratto, S. Daigle, and R. Longland, *Phys. Rev. C* **81** 045801 (2010).
[23] A. I. Karakas, M. A. Lugaro, M. Wiescher, J. Goörres, and C. Ugalde, *Astrophys. J.* **643**, 471 (2006).
[24] B. L. Berman, R. L. van Hemert, and C. D. Bowman, *Phys. Rev. Lett.* **23**, 386 (1969).
[25] H. W. Drotleff, A. Denker, J. W. Hammer, H. Knee, S. Küchler, D. Streit, C. Rolfs, and H. P. Trautvetter, *Z. Phys. A* **338**, 367 (1991).
[26] V. Harms, K.-L. Kratz, and M. Wiescher, *Phys. Rev. C* **43**, 2849 (1991).
[27] H. W. Drotleff, A. Denker, H. Knee, M. Soine, G. Wolf, J. W. Hammer, U. Greife, C. Rolfs, and H. P. Trautvetter, *Astrophys. J.* **414**, 735 (1993).
[28] H. R. Weller, M. W. Ahmed, H. Gao, W. Tornow, Y. K. Wu, M. Gai, and R. Miskimen, *Prog. Part. Nucl. Phys.* **62**, 257 (2009).
[29] L. C. Biedenharn and M. E. Rose, *Rev. Mod. Phys.* **25**, 729 (1953).
[30] R. Longland, C. Iliadis, and A. I. Karakas, *Phys. Rev. C* **85** 065809 (2012).